

## VERITAS Search for VHE Gamma-ray Emission from Dwarf Spheroidal Galaxies

V. A. Acciari<sup>1</sup>, T. Arlen<sup>2</sup>, T. Aune<sup>3</sup>, M. Beilicke<sup>4</sup>, W. Benbow<sup>1</sup>, D. Boltuch<sup>5</sup>,  
S. M. Bradbury<sup>6</sup>, J. H. Buckley<sup>4</sup>, V. Bugaev<sup>4</sup>, K. Byrum<sup>7</sup>, A. Cannon<sup>8</sup>, A. Cesarini<sup>9</sup>,  
J. L. Christiansen<sup>10</sup>, L. Ciupik<sup>11</sup>, W. Cui<sup>12</sup>, R. Dickherber<sup>4</sup>, C. Duke<sup>13</sup>, J. P. Finley<sup>12</sup>,  
G. Finnegan<sup>14</sup>, A. Furniss<sup>3</sup>, N. Galante<sup>1</sup>, S. Godambe<sup>14</sup>, J. Grube<sup>11</sup>, R. Guenette<sup>15</sup>,  
G. Gyuk<sup>11</sup>, D. Hanna<sup>15</sup>, J. Holder<sup>5</sup>, C. M. Hui<sup>14</sup>, T. B. Humensky<sup>16</sup>, A. Imran<sup>17</sup>,  
P. Kaaret<sup>18</sup>, N. Karlsson<sup>11</sup>, M. Kertzman<sup>19</sup>, D. Kieda<sup>14</sup>, A. Konopelko<sup>20</sup>, H. Krawczynski<sup>4</sup>,  
F. Krennrich<sup>17</sup>, G. Maier<sup>15,11</sup>, S. McArthur<sup>4</sup>, A. McCann<sup>15</sup>, M. McCutcheon<sup>15</sup>,  
P. Moriarty<sup>21</sup>, R. A. Ong<sup>2</sup>, A. N. Otte<sup>3</sup>, D. Pandel<sup>18</sup>, J. S. Perkins<sup>1</sup>, M. Pohl<sup>17,15</sup>, J. Quinn<sup>8</sup>,  
K. Ragan<sup>15</sup>, L. C. Reyes<sup>22</sup>, P. T. Reynolds<sup>23</sup>, E. Roache<sup>1</sup>, H. J. Rose<sup>6</sup>, M. Schroedter<sup>17</sup>,  
G. H. Sembroski<sup>12</sup>, G. Demet Senturk<sup>24</sup>, A. W. Smith<sup>7</sup>, D. Steele<sup>11,10</sup>, S. P. Swordy<sup>16</sup>,  
G. Tešić<sup>15</sup>, M. Theiling<sup>1</sup>, S. Thibadeau<sup>4</sup>, A. Varlotta<sup>12</sup>, V. V. Vassiliev<sup>2</sup>, S. Vincent<sup>14</sup>,  
R. G. Wagner<sup>7</sup>, S. P. Wakely<sup>16</sup>, J. E. Ward<sup>8</sup>, T. C. Weekes<sup>1</sup>, A. Weinstein<sup>2</sup>,  
T. Weisgarber<sup>16</sup>, D. A. Williams<sup>3</sup>, S. Wissel<sup>16</sup>, M. D. Wood<sup>2</sup>, B. Zitzer<sup>12</sup>

rgwcdf@hep.anl.gov

---

<sup>1</sup>Fred Lawrence Whipple Observatory, Harvard-Smithsonian Center for Astrophysics, Amado, AZ 85645, USA

<sup>2</sup>Department of Physics and Astronomy, University of California, Los Angeles, CA 90095, USA

<sup>3</sup>Santa Cruz Institute for Particle Physics and Department of Physics, University of California, Santa Cruz, CA 95064, USA

<sup>4</sup>Department of Physics, Washington University, St. Louis, MO 63130, USA

<sup>5</sup>Department of Physics and Astronomy and the Bartol Research Institute, University of Delaware, Newark, DE 19716, USA

<sup>6</sup>School of Physics and Astronomy, University of Leeds, Leeds, LS2 9JT, UK

<sup>7</sup>Argonne National Laboratory, 9700 S. Cass Avenue, Argonne, IL 60439, USA

<sup>8</sup>School of Physics, University College Dublin, Belfield, Dublin 4, Ireland

<sup>9</sup>School of Physics, National University of Ireland Galway, University Road, Galway, Ireland

<sup>10</sup>Physics Department, California Polytechnic State University, San Luis Obispo, CA 94307, USA

<sup>11</sup>Astronomy Department, Adler Planetarium and Astronomy Museum, Chicago, IL 60605, USA

<sup>12</sup>Department of Physics, Purdue University, West Lafayette, IN 47907, USA

<sup>13</sup>Department of Physics, Grinnell College, Grinnell, IA 50112-1690, USA

<sup>14</sup>Department of Physics and Astronomy, University of Utah, Salt Lake City, UT 84112, USA

<sup>15</sup>Physics Department, McGill University, Montreal, QC H3A 2T8, Canada

<sup>16</sup>Enrico Fermi Institute, University of Chicago, Chicago, IL 60637, USA

<sup>17</sup>Department of Physics and Astronomy, Iowa State University, Ames, IA 50011, USA

<sup>18</sup>Department of Physics and Astronomy, University of Iowa, Van Allen Hall, Iowa City, IA 52242, USA

<sup>19</sup>Department of Physics and Astronomy, DePauw University, Greencastle, IN 46135-0037, USA

<sup>20</sup>Department of Physics, Pittsburg State University, 1701 South Broadway, Pittsburg, KS 66762, USA

<sup>21</sup>Department of Life and Physical Sciences, Galway-Mayo Institute of Technology, Dublin Road, Galway, Ireland

<sup>22</sup>Kavli Institute for Cosmological Physics, University of Chicago, Chicago, IL 60637, USA

<sup>23</sup>Department of Applied Physics and Instrumentation, Cork Institute of Technology, Bishopstown, Cork, Ireland

<sup>24</sup>Columbia Astrophysics Laboratory, Columbia University, New York, NY 10027, USA

<sup>II</sup>Now at DESY, Platanenallee 6, 15738 Zeuthen, Germany

<sup>U</sup>Now at Institut für Physik und Astronomie, Universität Potsdam, 14476 Potsdam-Golm, Germany;

## ABSTRACT

Indirect dark matter searches with ground-based gamma-ray observatories provide an alternative for identifying the particle nature of dark matter that is complementary to that of direct search or accelerator production experiments. We present the results of observations of the dwarf spheroidal galaxies Draco, Ursa Minor, Boötes 1, and Willman 1 conducted by the Very Energetic Radiation Imaging Telescope Array System (VERITAS). These galaxies are nearby dark matter dominated objects located at a typical distance of several tens of kiloparsecs for which there are good measurements of the dark matter density profile from stellar velocity measurements. Since the conventional astrophysical background of very high energy gamma rays from these objects appears to be negligible, they are good targets to search for the secondary gamma-ray photons produced by interacting or decaying dark matter particles. No significant gamma-ray flux above 200 GeV was detected from these four dwarf galaxies for a typical exposure of  $\sim 20$  hours. The 95% confidence upper limits on the integral gamma-ray flux are in the range  $0.4 - 2.2 \times 10^{-12}$  photons  $\text{cm}^{-2}\text{s}^{-1}$ . We interpret this limiting flux in the context of pair annihilation of weakly interacting massive particles (WIMPs) and derive constraints on the thermally averaged product of the total self-annihilation cross section and the relative velocity of the WIMPs ( $\langle\sigma v\rangle \lesssim 10^{-23}$   $\text{cm}^3 \text{s}^{-1}$  for  $m_\chi \gtrsim 300$   $\text{GeV}/c^2$ ). This limit is obtained under conservative assumptions regarding the dark matter distribution in dwarf galaxies and is approximately three orders of magnitude above the generic theoretical prediction for WIMPs in the minimal supersymmetric standard model framework. However significant uncertainty exists in the dark matter distribution as well as the neutralino cross sections which under favorable assumptions could further lower this limit.

*Subject headings:* gamma rays: observations — dark matter — galaxies: dwarf

## 1. Introduction

The existence of astrophysical non-baryonic dark matter (DM) has been established by its gravitational effects on a wide range of spatial scales. Perhaps the most compelling evi-

---

DESY, Platanenallee 6, 15738 Zeuthen, Germany

$\diamond$ Now at Los Alamos National Laboratory, MS H803, Los Alamos, NM 87545

dence for the existence of weakly interacting particle dark matter comes from observations of colliding galaxy clusters in which the baryonic matter in the form of X-ray emitting gas is separated from the source of the gravitational potential detected through gravitational lensing (Clowe *et al.* 2006; Bradač *et al.* 2008). However, despite the well-established presence of DM in the universe, its particle nature is unknown.

The quest to understand the nature of DM draws upon research in cosmology, particle physics, and astroparticle physics with direct and indirect detection experiments (Bergström 2000; Bertone *et al.* 2005). In this paper we focus on the indirect search for very high energy (VHE, Energy  $> 100$  GeV) gamma rays resulting from the interaction or decay of DM particles in astrophysical objects in which the gravitational potential is dominated by DM.

Among many theoretical candidates for the DM particle (Taoso *et al.* 2008), a weakly interacting massive particle (WIMP) is among the best motivated. A thermal relic of the early universe with an interaction cross section on the weak scale will naturally produce the present-day DM density if the particle has a weak-scale mass (Lee & Weinberg 1977; Dicus *et al.* 1977) ( $\Omega_{DM}h^2 = 0.1099 \pm 0.0062$  (WMAP only),  $\Omega_{DM}h^2 = 0.1131 \pm 0.0034$  (WMAP + Baryon Acoustic Oscillations + Type Ia Supernovae), where  $\Omega_{DM}$  is the ratio of dark matter density to the critical density for a flat universe and  $h$  is a dimensionless quantity defined as the Hubble constant,  $H_0$ , normalized to  $100\text{km s}^{-1}\text{Mpc}^{-1}$  (Komatsu *et al.* 2009)). Several candidates for WIMPs are predicted in extensions to the standard model of particle physics, for example, the neutralino from supersymmetry (Ellis *et al.* 1984) and the Kaluza-Klein particle in theories of universal extra dimensions (Servant & Tait 2003; Bertone *et al.* 2003). Both neutralinos and Kaluza-Klein particles are predicted to have a mass in the range of a few tens of  $\text{GeV}/c^2$  to possibly a few  $\text{TeV}/c^2$ .

The self-annihilation of WIMPs produces a unique spectral signature of secondary gamma rays which is expected to significantly deviate from the standard power-law behavior observed in most conventional astrophysical sources of VHE gamma rays and would have a cutoff at the WIMP mass. In addition, it could exhibit a monoenergetic line at the WIMP mass or a considerable enhancement of gamma-ray photons at the endpoint of the spectrum due to the internal bremsstrahlung effect (Bringmann *et al.* 2008). Observation of these spectral signatures combined with the spatial distribution of the gamma-ray flux from an astrophysical source is a unique capability of indirect DM searches utilizing gamma rays.

Nearby astrophysical objects with the highest dark matter density are natural candidates for indirect DM searches. While the Galactic Center is likely to be the brightest source of annihilation radiation (e.g. see Bergström *et al.* 1998), VHE gamma-ray measurements reveal a bright gamma-ray source at the center which constitutes a large astrophysical background (Aharonian *et al.* 2006a). Other possible bright sources are expected to be the

cores of nearby large galaxies such as M31 or halos around galactic intermediate mass black holes, should they exist, where adiabatic compression of dark matter halos could result in a large enhancement in the annihilation signal, in some cases already exceeding experimental bounds (Bringmann *et al.* 2009a; Bertone *et al.* 2009). However, in these regions, the DM density profiles are poorly constrained and, in the case of nearby galaxies, conventional astrophysical VHE sources can generate backgrounds for DM annihilation searches. In contrast, the satellite dwarf spheroidal galaxies (dSphs) of the Milky Way are attractive targets for indirect dark matter searches due to their proximity (20-100 kpc) and relatively well-constrained DM profiles derived from stellar kinematics. They, in fact, may be the brightest sources for annihilation radiation after the Galactic Center (Bullock *et al.* 2009). The general lack of active or even recent star formation in most dSphs implies that there is little background from conventional astrophysical VHE processes as has been observed in the Milky Way Galactic Center (Kosack *et al.* 2004; Aharonian *et al.* 2006b, 2009). The growing class of nearby dSphs discovered by recent all-sky surveys (York *et al.* 2000; Belokurov *et al.* 2007) increases the probability of finding an object for which the halo density is sufficient to yield a detectable gamma-ray signal.

In this paper, we report on an indirect DM search for gamma rays from four dSphs: Draco, Ursa Minor, Boötes 1 and Willman 1, carried out using the Very Energetic Radiation Imaging Telescope Array System (VERITAS). After a brief summary of the properties of the observational targets and previous VHE observations in Section 2, we describe the VERITAS instrument, the data set, and the analysis techniques in Section 3. Sections 4 and 5 are devoted to the discussion of the results and their interpretation in terms of constraints on the WIMP parameter space. We conclude in Section 6 with a discussion of the opportunities for indirect DM detection by future ground-based gamma-ray instrumentation.

## 2. Observational Targets

Three of the dSphs forming the subject of this paper, Draco, Ursa Minor, and Willman 1, have been identified as the objects within the dSph class with potentially the highest gamma-ray self-annihilation flux, e.g. see Strigari *et al.* (2007, 2008). The modeling of the DM distribution of these galaxies usually is based on stellar kinematics assuming a spherically symmetric stellar population and an NFW profile for DM (Navarro *et al.* 1997) characterized by two parameters: the scale radius  $r_s$  and scale density  $\rho_s$ ,

$$\rho(r) = \rho_s \left( \frac{r}{r_s} \right)^{-1} \left( 1 + \frac{r}{r_s} \right)^{-2}. \quad (1)$$

Table 1: Properties of the four dSphs. Preferred values for DM halo parameters,  $\rho_s$  and  $r_s$ , which are defined in the text are taken from Strigari *et al.* (2007) and Bringmann *et al.* (2009b). Values for  $L_V$ , the visual luminosity, and  $r_h$ , the half-light radius are taken from Walker *et al.* (2009).  $R_d$  is heliocentric distance of the dSph. The calculation of the dimensionless line of sight integral,  $J$ , which is normalized to the critical density squared times the Hubble radius ( $3.832 \times 10^{17} \text{GeV}^2 \text{cm}^{-5}$ ), is explained in Section 5. The  $J$  value for Boötes was calculated by G.D. Martinez and J.S. Bullock. As explained in the text, the elongation of Boötes and the relative lack of stellar kinematic data lead to large uncertainties for  $r_s$  or  $\rho_s$  and no values are provided in this case.

Quantity	Draco	Ursa Minor	Boötes 1	Willman 1
$\alpha$ [J2000.0]	$17^h 20^m 12.4^s$	$15^h 09^m 11.3^s$	$14^h 00^m 06^s$	$10^h 49^m 22.3^s$
$\delta$ [J2000.0]	$57^\circ 54' 55''$	$67^\circ 12' 52''$	$14^\circ 30' 00''$	$51^\circ 03' 03''$
$L_V$ [ $L_\odot$ ]	$(2.7 \pm 0.4) \times 10^5$	$(2.0 \pm 0.9) \times 10^5$	$(3.0 \pm 0.6) \times 10^4$	$(1.0 \pm 0.7) \times 10^3$
$r_h$ [pc]	$221 \pm 16$	$150 \pm 18$	$242 \pm 21$	$25 \pm 6$
$R_d$ [kpc]	80	66	62	38
$\rho_s$ [ $M_\odot/\text{kpc}^3$ ]	$4.5 \times 10^7$	$4.5 \times 10^7$	—	$4 \times 10^8$
$r_s$ [kpc]	0.79	0.79	—	0.18
$J(\rho_s, r_s)$	4	7	3	22

The properties of these galaxies including constraints on  $r_s$  and  $\rho_s$  as found in Strigari *et al.* (2007) and Strigari *et al.* (2008) are summarized in Table 1.

The Draco dSph is one of the most frequently studied objects for indirect DM detection (Baltz *et al.* 2000; Tyler 2002; Evans *et al.* 2004; Colafrancesco *et al.* 2007; Sánchez-Conde *et al.* 2007; Strigari *et al.* 2007, 2008; Bringmann *et al.* 2009b). It has an approximately spherically symmetric stellar distribution (Irwin & Hatzidimitriou 1995) with total luminosity of the order of  $10^5 L_\odot$  (Piatek *et al.* 2002). The large spectroscopic data set available for this object (Wilkinson *et al.* 2004; Muñoz *et al.* 2005; Walker *et al.* 2007) tightly constrains its DM distribution profile. Draco is consistent with an old low-metallicity ( $[\text{Fe}/\text{H}] = -1.8 \pm 0.2$ ) stellar population with no significant star formation over the last 2 Gyrs (Aparicio *et al.* 2001). Draco previously has been observed at VHE energies by the STACEE observatory (Driscoll *et al.* 2008), the Whipple 10m telescope (Wood *et al.* 2008), and the MAGIC telescope (Albert *et al.* 2008).

The Ursa Minor dSph has a distance and inferred DM content similar to those of Draco. There is no evidence of young or intermediate age stellar populations in Ursa Minor (Shetrone *et al.* 2001). Photometric studies of this object have found evidence for significant structures in the stellar distribution in the central  $10'$  (Bellazzini *et al.* 2002; Kleyana *et al.* 2003) and an extratidal stellar population (Palma *et al.* 2003). These unusual morphological characteristics could be evidence of possible tidal interaction with the Milky Way, velocity projection effects along the line of sight, or the presence of fluctuations in the DM induced gravitational potential (Kleyana *et al.* 2003). In fact, such confusing factors are present in most dSph galaxies. Ursa Minor was previously studied at VHE energies by the Whipple 10m telescope (Wood *et al.* 2008).

The recently discovered dSph Boötes 1 (Belokurov *et al.* 2006) shows evidence for elongation of the stellar profile. N-Body simulations can not reproduce the observed velocity dispersion without a dominant contribution from DM. In addition, modeling of the tidal interaction effects between Boötes 1 and the Milky Way do not provide an adequate explanation for the elongation of this system suggesting a non-spherically symmetric distribution of DM in the Boötes progenitor (Fellhauer *et al.* 2008). Given the stellar kinematical data is based on about 30 stars, the scale radius and density of the NFW profile have large uncertainty as well as significant degeneracy. Thus, values for  $r_s$  and  $\rho_s$  are unavailable in the literature. The modeling of Boötes 1 was done by G.D. Martinez and J.S. Bullock (2009, private communication) for a range of NFW fits. The methodology is described in Martinez *et al.* (2009); Abdo *et al.* (2010). They produce a probability density function (pdf) for  $J$ , the astrophysical contribution to the flux (see Section 5), which is approximately Gaussian in  $\log(J)$ . The value given in Table 1 represents  $J$  at the peak of the pdf which is approx-

imately the mean of the distribution. The estimates of the age of the stellar population and metallicity suggest similarity with the old and metal-poor ( $[\text{Fe}/\text{H}] \sim -2.5 - -2.1$ ) stellar distribution of M92 (Belokurov *et al.* 2006; Muñoz *et al.* 2006; Martin *et al.* 2007). To date, no other VHE gamma-ray observations have been reported for this object.

Together with Boötes 1, Willman 1 belongs to the new class of low surface brightness dSphs recently discovered by the Sloan Digital Sky Survey (Willman *et al.* 2005). Willman 1 is one of the smallest ( $r_h \sim 25$  pc) and least luminous ( $L_V \sim 10^3 L_\odot$ ) dSphs known. Its half-light radius and absolute magnitude suggest that it may be an intermediate object between dwarf galaxies and globular clusters (Belokurov *et al.* 2007). Due to the small kinematic sample of stars available for this object, the constraints on the DM halo parametrization are poor (Strigari *et al.* 2008). Latest estimates of the metallicity suggest a low value of  $[\text{Fe}/\text{H}]$  which is consistent with the observed trend of decreasing metallicity for fainter dSphs (Siegel *et al.* 2008). The MAGIC collaboration has recently reported the results of the observations of Willman 1 (Aliu *et al.* 2009).

### 3. Data and Analysis

#### 3.1. The VERITAS Observatory

The VERITAS observatory is an array of four 12m imaging atmospheric Cherenkov telescopes (IACTs) located at the Fred Lawrence Whipple Observatory ( $31^\circ 57' \text{N}$   $111^\circ 37' \text{W}$ ) in southern Arizona at an altitude of 1.27 km above sea level (Weekes *et al.* 2002). The observatory is sensitive over an energy range of 150 GeV to 30 TeV with an energy resolution of 10-20% and an angular resolution (68% containment) of  $< 0.14^\circ$  per event. For the measurements reported here, VERITAS had a point source sensitivity capable of detecting gamma rays with a flux of 5% (1%) of the Crab Nebula flux above 300 GeV at five standard deviations in  $< 2.5$  ( $< 50$ ) hours at  $20^\circ$  zenith angle. During summer, 2009 subsequent to the four dSph observations, the array configuration was changed, improving the point source sensitivity. Further technical description of the VERITAS observatory can be found in Acciari *et al.* (2008).

#### 3.2. Data

Observations of the Draco, Ursa Minor, Boötes 1, and Willman 1 dSphs were performed during 2007-2009 (see Table 2). Observations were taken in “wobble” mode (Berge *et al.* 2007) with the source offset by  $0.5^\circ$  from the center of the field of view in order to obtain



source and background measurement within the same observation. The direction of the offset was alternated between north, south, east, and west to minimize systematic errors. *Reflected* background regions are defined within the field of view at the same radius with respect to the camera center as that of the targeted dwarf galaxy. Observations were made with varying atmospheric conditions during moonless periods of the night. Data were quality selected for analysis based on the stability of the cosmic-ray trigger rate and the rms temperature fluctuations observed by an FIR camera viewing the sky in the vicinity of the observed target ( $\leq 0.3^\circ\text{C}$ ). The total exposure on each source is given in Table 2.

### 3.3. Analysis

Data reduction follows the methods described in Acciari *et al.* (2008). A brief outline of the analysis flow follows. Images recorded by each of the VERITAS telescopes are characterized by a second moment analysis giving the Hillas parameters (Hillas 1985). A stereoscopic analysis of the image parameters is used to reconstruct the gamma ray arrival direction and shower core position. The background of cosmic rays is reduced by a factor of  $> 10^5$  utilizing cuts on the reconstructed arrival direction ( $\theta^2 < 0.013 \text{ deg}^2$ ) and the image shape parameters, mean scaled width and length ( $0.05 \leq msw \leq 1.16$  and  $0.05 \leq msl \leq 1.36$ ). The image distance from the center of the camera is required to be less than  $1.43^\circ$  to avoid truncation effects at the edge of the  $3.5^\circ$  field of view. The integrated charge recorded in at least two telescopes is further required to be  $> 75$  photoelectrons (400 digital counts) which effectively sets the energy threshold of the analysis to be above  $\sim 200$  GeV depending on the zenith angle. The energy threshold quoted in our analyses is taken to be the energy at which the differential detection rate of gamma rays from the Crab Nebula peaks. The cuts applied in this analysis were optimized to maximize significance of the detection for a hypothetical source with a power-law spectrum ( $dF/dE = 3.2 \times 10^{-12} (E/\text{TeV})^{-2.5} \text{ cm}^{-2} \text{ s}^{-1} \text{ TeV}^{-1}$ ) corresponding to 3% of the Crab Nebula flux. Two independent data analysis packages were used to analyze the data and yielded consistent results.

Table 2: Summary of observation periods and exposures of dSphs by VERITAS.

Source	Period	Exposure [hr]	Zenith Angle [°]
Draco	2007 Apr-May	18.38	26 – 51
Ursa Minor	2007 Feb-May	18.91	35 – 46
Boötes 1	2009 Apr-May	14.31	17 – 29
Willman 1	2007 Dec-2008 Feb	13.68	19 – 28

The significance of the detection was calculated by comparing the counts in the source region to the expected background counts. The background in the source region is estimated using the *reflected region* model. In this model circular background regions, here of angular radius  $0.115^\circ$ , are defined with an offset from the camera center equal to that of the putative source. Eleven background regions can be accommodated within the VERITAS field of view. The absence of bright stars within any of the four dSph pointings allows all eleven regions to be used in the background count estimation. The significance of any signal is computed using the Li and Ma method (Li & Ma 1983, eqn. 17).

#### 4. Results

Table 3 summarizes the results for each of the four dSphs. The effective energy threshold for each of the targets changes primarily due to the average zenith angle of observations. The table shows the average effective collecting area for gamma rays as calculated from a sample of simulated gamma-ray showers. No significant excesses of counts above background were detected from these observations. The 95% confidence level upper limits on the gamma-ray integral flux were calculated using the bounded profile likelihood ratio statistic developed by Rolke *et al.* (2005).

As we have noted, Draco, Ursa Minor, and Willman I have been observed by other IACTs and we briefly compare our flux limits to the other observations. For Draco, STACEE (Driscoll *et al.* 2008) finds a spectral limit of less than  $1.6 \times 10^{-13} \left(\frac{E}{200\text{GeV}}\right)^{-2.2} \text{cm}^{-2}\text{s}^{-1}\text{GeV}^{-1}$ . The MAGIC flux limit (Albert *et al.* 2008) from observation of Draco is  $1.1 \times 10^{-11} \text{cm}^{-2}\text{s}^{-1}$  above a threshold of 140 GeV. MAGIC also has set flux limits for Willman 1 in the range  $5.7 - 9.9 \times 10^{-12} \text{cm}^{-2}\text{s}^{-1}$  above 100 GeV based on several benchmark models (Aliu *et al.* 2009), compared to our limit of  $1.17 \times 10^{-12} \text{cm}^{-2}\text{s}^{-1}$  above a threshold of 320 GeV. The limits for the VERITAS observations of Draco and Ursa Minor are an improvement of about a factor of 40 over the earlier observations of the group on the Whipple 10m IACT (Wood *et al.* 2008).

Figure 1 shows the upper limits on the differential spectral energy density ( $E^2 d\phi/dE$ ) as a function of energy. The upper limits were derived with four equidistant log energy bins per decade requiring 95% C.L. in each bin.

## 5. Limits on WIMP Parameter Space

The differential flux of gamma rays from WIMP self-annihilation is given by

$$\frac{d\phi(\Delta\Omega)}{dE} = \frac{\langle\sigma v\rangle}{8\pi m_\chi^2} \left[ \frac{dN(E, m_\chi)}{dE} \right] \int_{\Delta\Omega} d\Omega \int \rho^2(\lambda, \Omega) d\lambda, \quad (2)$$

where  $\langle\sigma v\rangle$  is the thermally averaged product of the total self-annihilation cross section and the velocity of the WIMP,  $m_\chi$  is the WIMP mass,  $dN(E, m_\chi)/dE$  is the differential gamma-ray yield per annihilation,  $\Delta\Omega$  is the observed solid angle around the dwarf galaxy center,  $\rho$  is the DM mass density, and  $\lambda$  is the line-of-sight distance to the differential integration volume. The astrophysical contribution to the flux can be expressed by the dimensionless factor  $J$

$$J(\Delta\Omega) = \left( \frac{1}{\rho_c^2 R_H} \right) \int_{\Delta\Omega} d\Omega \int \rho^2(\lambda, \Omega) d\lambda, \quad (3)$$

which has been normalized to the product of the square of the critical density,  $\rho_c = 9.74 \times 10^{-30} \text{g cm}^{-3}$  and the Hubble radius,  $R_H = 4.16 \text{ Gpc}$  following Wood *et al.* (2008).

Based on equation 2, the upper limits on the gamma-ray rate,  $R_\gamma(95\% \text{ C.L.})$ , constrain the WIMP parameter space  $(m_\chi, \langle\sigma v\rangle)$  according to

$$\begin{aligned} \frac{R_\gamma(95\% \text{ C.L.})}{\text{hr}^{-1}} &> \frac{J}{1.09 \times 10^4} \left( \frac{\langle\sigma v\rangle}{3 \times 10^{-26} \text{cm}^3 \text{s}^{-1}} \right) \\ &\times \int_0^\infty \frac{A(E)}{5 \times 10^8 \text{cm}^2} \left( \frac{300 \text{ GeV}/c^2}{m_\chi} \right)^2 \frac{EdN/dE(E, m_\chi) dE}{10^{-2} E}, \end{aligned} \quad (4)$$

where  $A(E)$  is the energy-dependent gamma-ray collecting area. The expression has been cast as a product of dimensionless factors with the variables normalized to representative quantities, e.g. the cross section times velocity is normalized to  $3 \times 10^{-26} \text{cm}^3 \text{s}^{-1}$  which is a rough generic prediction for  $\langle\sigma v\rangle$  for a WIMP thermal relic in the absence of coannihilations for  $m_\chi > 100 \text{ GeV}/c^2$  (c.f. figure 2). The main contribution to the integral comes from the energy range in the vicinity of the energy threshold ( $E \simeq 300 \text{ GeV}$  for observations in this paper) where  $A(E)$  changes rapidly. For VERITAS the effective area at 300 GeV is  $\sim 6 \times 10^8 \text{cm}^2$ . For a representative MSSM model,  $EdN/dE$  at 300 GeV is a function of neutralino mass,  $m_\chi$ , and it changes in the range  $10^{-2} - 10^{-1}$  for  $m_\chi$  from 300 GeV/ $c^2$  to a few TeV/ $c^2$ . Although  $EdN/dE$  is a rapid function of  $m_\chi$ , this dependence is nearly compensated by the  $(300 \text{ GeV}/c^2/m_\chi)^2$  prefactor. The product of these two contributions and, consequently, the overall integral value, is weakly dependent on the neutralino mass within the indicated range and is on the order of 1. It is evident from the inequality (Equation 4) that for a typical upper limit on the detection rate of 1 gamma ray per hour, significantly constraining upper limits on  $\langle\sigma v\rangle$  could be established if  $J$  is on the order of  $10^4$ .

Because the factor,  $J$ , is proportional to the DM density squared, it is subject to considerable uncertainty in its experimental determination. For example, the mass of a DM halo is determined by the interaction of a galaxy with its neighbors and is concentrated in the outer regions of the galaxy. Unlike the DM halo mass, the neutralino annihilation flux is determined by the inner regions of the galaxy where the density is the highest. For these regions the stellar kinematic data do not fully constrain the DM density profile due to limited statistics. Various parametrizations of the DM mass density profile have been put forward (Navarro *et al.* 1997; Kazantzidis *et al.* 2004; de Blok *et al.* 2001; Burkert 1995) based on empirical fits and studies of simulated Cold Dark Matter (CDM) halos. We adopt the assumption of the NFW profile (Navarro *et al.* 1997) given in Equation 1 which describes a smooth distribution of DM with a single spatial scale factor  $r_s$ . The astrophysical factor,  $J$ , is then given by

$$J(\Delta\Omega) = \left( \frac{2\pi\rho_s^2}{\rho_c^2 R_H} \right) \int_{\cos(0.115^\circ)}^1 \int_{\lambda_{min}}^{\lambda_{max}} \left( \frac{r(\lambda)}{r_s} \right)^{-2} \left[ 1 + \left( \frac{r(\lambda)}{r_s} \right) \right]^{-4} d\lambda d(\cos\theta), \quad (5)$$

where the lower integration bound of  $0.115^\circ$  corresponds to the size of the signal integration region. The galactocentric distance,  $r(\lambda)$ , is determined by

$$r(\lambda) = \sqrt{\lambda^2 + R_{dSph}^2 - 2\lambda R_{dSph} \cos\theta}, \quad (6)$$

where  $\lambda$  is the line of sight distance and  $R_{dSph}$  is the distance of the dwarf galaxy from the Earth.

Although the integration limits,  $\lambda_{min}$  and  $\lambda_{max}$ , are determined by the tidal radius of the dSph ( $r_t = 7$  kpc was used for these calculations) (Sánchez-Conde *et al.* 2007), the main contribution to  $J(\Delta\Omega)$  comes from the regions  $r < r_s \ll r_t$  and therefore the choice of  $r_t$  negligibly affects the  $J$  value. The main uncertainty for  $J$  computation is due to the choice of  $\rho_s$  and  $r_s$ . For Draco and Ursa Minor,  $\rho_s$  and  $r_s$  are taken as the midpoints of the range from Strigari *et al.* (2007). For Willman 1,  $\rho_s$  and  $r_s$  are adopted from Bringmann *et al.* (2009b). The  $J$  value Boötes 1 was calculated by Martinez and Bullock as discussed in section 2. The summary of the  $J$  values calculated for each object is given in Table 1.

An estimated value of  $J$  of order 10 is representative for all observed dSphs, which is three orders of magnitude below the value needed to constrain generic WIMP models with  $m_\chi \gtrsim 100$  GeV/ $c^2$ . Figure 2 shows the exclusion region in the  $(m_\chi, \langle\sigma v\rangle)$  parameter space due to the observations reported in this paper. MSSM models shown in the figure were produced with a random scan of the 7-parameter phase space defined in the DarkSUSY package (Gondolo *et al.* 2004) with the additional WMAP (Spergel *et al.* 2007) constraint on the cosmological DM energy density.

Several astrophysical factors can increase the value of  $J$  as compared to the conservative estimates given in Table 1. First, the inner asymptotic behavior of the DM density may be steeper than  $\propto r^{-1}$  predicted by the NFW profile due to unaccounted physical processes at small spatial scales. The extreme assumption would be the Moore profile (Moore *et al.* 1999)  $\propto r^{-1.5}$  asymptotically which generates a logarithmically divergent self-annihilation flux indicating that another physical process, for example self-annihilation, would limit the DM density in the central regions of the galaxy. A second factor that would increase the value of  $J$  is deviations of the DM distribution from a smooth average profile (substructures). CDM N-body simulations predict substructures in DM halos (Silk & Stebbins 1993; Diemand *et al.* 2005, 2007) and the effects on the DM self-annihilation have been studied in these simulations. In general any regions of DM overdensity will enhance the self-annihilation flux; the cumulative effect of these enhancements is usually referred to as the boost factor. Strigari *et al.* (2007) find a maximum boost factor of order  $10^2$  while a more detailed calculation that accounts for the particle properties of the neutralino during formation of DM halos suggests boost factors of order 10 and below (Martinez *et al.* 2009). Thus, present generation IACTs could be as close as two orders of magnitude in sensitivity from constraining generic MSSM models.

Two effects related to the properties of the WIMP particle may improve the chances of the detection of neutralino self-annihilation by ground-based gamma-ray observatories. Internal bremsstrahlung gamma rays produced in neutralino self-annihilation recently calculated by Bringmann *et al.* (2008) can significantly enhance  $dN/dE$  at the energies comparable to  $m_\chi$  for some MSSM models due to the absence of the helicity suppression factor. Effectively this increases the value of the integral in Equation 4, especially for the higher mass neutralino models. In addition, the  $\langle\sigma v\rangle$  for self-annihilation at the present cosmological time may be considerably larger than at the time of WIMP decoupling due to a velocity-dependent term in the cross-section and the reduction of the kinetic energy of the WIMP due to the cosmological expansion of the universe (Robertson & Zentner 2009; Pieri *et al.* 2009).

## 6. Conclusions

We have carried out a search for VHE gamma rays from four dSphs: Draco, Ursa Minor, Boötes 1, and Willman 1, as part of an indirect DM search program at the VERITAS observatory. The dSphs were selected for proximity to Earth and for favorable estimates of the J factor based on stellar kinematics data. No significant gamma-ray excess was observed from the four dSphs, and the derived upper limits on the gamma-ray flux constrain the  $\langle\sigma v\rangle$

for neutralino pair annihilation as a function of neutralino mass to be  $\lesssim 10^{-23} \text{ cm}^3 \text{ s}^{-1}$  for  $m_\chi \gtrsim 300 \text{ GeV}/c^2$ . The obtained  $\langle\sigma v\rangle$  limits are three orders of magnitude above generic predictions for MSSM models assuming an NFW DM density profile, no boost factor, and no additional particle-related gamma-ray flux enhancement factors. Should the neglected effects be included, the constraints on  $\langle\sigma v\rangle$  in the most optimistic regime could be pushed to  $\lesssim 10^{-25} \text{ cm}^3 \text{ s}^{-1}$ .

To begin confronting the predictions of generic MSSM models through observation of presently known dSphs, future ground-based observatories will need a sensitivity at least an order of magnitude better than present-day instruments. The list of dSphs favorable for observations of DM self-annihilation has grown over the last years by a factor of roughly two, and it is anticipated that newly discovered dSphs may offer a larger factor  $J$ . The ongoing sky survey conducted by the Fermi Gamma-ray Space Telescope (FGST) may also identify nearby higher DM density substructures within the MW galaxy which could be followed up by the IACT observatories. Typical current exposures accumulated on dSphs by IACTs are of order 20 hours, and ongoing observing programs could feasibly increase the depth of these observations by a factor of 10 (a sensitivity increase of  $\sim 3$ ). Improvements in background rejection are anticipated to increase sensitivity by an additional 20-50%. The soon-to-be-operational upgrades, MAGIC-II and HESS-II, as well as a planned VERITAS upgrade will reduce the energy threshold and consequently increase the  $dN/dE$  contribution by a factor as large as 10 thus providing an additional sensitivity improvement. With all these factors combined, the  $\langle\sigma v\rangle$  limits for  $m_\chi \gtrsim 300 \text{ GeV}/c^2$  will begin to rule out the most favorable MSSM models assuming a moderate boost factor. Next generation IACT arrays now being planned such as the Advanced Gamma-ray Imaging System (AGIS) <sup>1</sup> and the Cherenkov Telescope Array (CTA) <sup>2</sup> will provide an order of magnitude increase in sensitivity and lower the energy threshold by factor of  $\sim 2$  as compared to VERITAS. These instruments will be able to probe the bulk of the parameter space for generic MSSM models with  $m_\chi \simeq 300 \text{ GeV}/c^2$  without strong assumptions regarding potential flux enhancement factors.

This research is supported by grants from the US National Science Foundation, the US Department of Energy, and the Smithsonian Institution, by NSERC in Canada, by Science Foundation Ireland, and by STFC in the UK. We acknowledge the excellent work of the technical support staff at the FLWO and the collaborating institutions in the construction and operation of the instrument. V.V.V. acknowledges the support of the U.S. National Science Foundation under CAREER program (Grant No. 0422093).

---

<sup>1</sup><http://www.agis-observatory.org/>

<sup>2</sup><http://www.cta-observatory.org/>

## REFERENCES

- Abdo, A. A. *et al.* 2010 ApJ, 712, 147
- Acciari, V. A., *et al.* (VERITAS collaboration) 2008, ApJ, 679, 1427
- Aharonian, F. *et al.* (HESS collaboration) 2006a, A&A, 457, 899
- Aharonian, F. *et al.* (HESS collaboration) 2006b, Phys. Rev. Lett., 97, 221102
- Aharonian, F. *et al.* (HESS collaboration) 2009, A&A, 503, 817
- Albert, J. *et al.* (MAGIC collaboration) 2008, ApJ, 679, 428
- Aliu, E. *et al.* (MAGIC collaboration) 2009, ApJ, 697, 1299
- Aparicio, A., Carrera, R., & Martínez-Delgado, D. 2001, AJ, 122, 2524
- Baltz, E. A., Briot, C., Salati, P., Taillet, R., & Silk, J. 2000, Phys. Rev. D, 61, 023514
- Bellazzini, M., Ferraro, F. R., Origlia, L., Pancino, E., Monaco, L., & Olivia, E. 2002 AJ, 124, 3222
- Belokurov, V., *et al.* 2006, ApJ, 647, L111
- Belokurov, V., *et al.* 2007, ApJ, 654, 897
- Berge, D., Funk, S., & Hinton, J. 2007, A&A, 466, 1219
- Bergström, L., Ullio, P., Buckley, J. 1998, Astropart. Phys. 9, 137
- Bergström, L. 2000, Rep. on Prog. in Phys., 63, 793
- Bertone, G., Servant, G., & Sigl, G. 2003, Phys. Rev. D, 68, 044008
- Bertone, G., Hooper, D., & Silk, J. 2005, Phys. Rep., 405, 279
- Bertone, G., Fornasa, M., Taoso, M., & Zentner, A. R. 2009, New J. Phys., 11, 105016
- Bradač, M., Allen, S. W., Treu, T., Ebeling, H., Massey, R., Morris, R. G., von der Linden, A., & Applegate, D. 2008, ApJ, 687, 959
- Bringmann, T., Bergström, L., & Edsjö, J. 2008, J. High Energy Phys., JHEP01(2008)049
- Bringmann, T., Lavalle, J., & Salati, P. 2009a, Phys. Rev. Lett., 103, 161301

- Bringmann, T., Doro, M., & Fornasa, M. 2009b, *J. Cosmology Astropart. Phys.*, JCAP01(2009)016
- Burkert, A. 1995, *ApJ*, 447, L25
- Bullock, J. S. *et al.* 2009, arXiv:0902.3492
- Clowe, D., Bradač, M., Gonzalez, A. H., Markevitch, M., Randall, S. W., Jones, C., & Zaritsky, D. 2006, *ApJ*, 648, L109
- Colafrancesco, S., Profumo, S., & Ullio, P. 2007, *Phys. Rev. D*, 75, 023513
- de Blok, W. J. G., McGaugh, S. S., Bosma, A., & Rubin, V. C. 2001, *ApJ*, 552, L23
- Dicus, D. A., Kolb, E. W., Teplitz, V. L. 1977, *Phys. Rev. Lett.*, 39, 168
- Diemand, J., Moore, B., & Stadel, J. 2005, *Nature*, 433, 389
- Diemand, J., Kuhlen, M., & Madau, P. 2007, *ApJ*, 657, 262
- Driscoll, D. D. *et al.* (STACEE collaboration) 2008, *Phys. Rev. D*, 78, 087101
- Ellis, J., Hagelin, J. S., Nanopoulos, D. V., Olive, K., Srednicki, M. 1984, *Nucl. Phys. B*, 238, 453
- Evans, N. W., Ferrer, F., & Sarkar, S. 2004, *Phys. Rev. D*, 69, 123501
- Fellhauer, M., Wilkinson, M. I., Evans, N. W., Belokurov, V., Irwin, M. J., Gilmore, G., Zucker, D. B., & Kleyna, J. T. 2008, *MNRAS*, 385, 1095
- Gondolo, P., Edsjö, J., Ullio, P., Bergström, L., Schelke, M., & Baltz, E. A. 2004, *J. Cosmol. Astropart. Phys.*, JCAP07(2004)008
- Hillas, M. 1985, *Proc. 19<sup>th</sup> ICRC (La Jolla)*, 445
- Irwin, M., & Hatzidimitriou, D. 1995, *MNRAS*, 277, 1354
- Kazantzidis, S., Mayer, L., Mastrogiuseppe, C., Diemand, J., Stadel, J., & Moore, B. 2004 *ApJ*, 608, 663
- Kleyna, J. T., Wilkinson, M. I., Gilmore, G., & Evans, N. W. 2003, *ApJ*, 588, L21
- Komatsu, E. *et al.* 2009, *ApJS*, 180, 330
- Kosack, K. *et al.* (VERITAS collaboration) 2004, *ApJ*, 608, L97



- Lee, B. W., & Weinberg, S. 1977, *Phys. Rev. Lett.*, 39, 165
- Li, T-P., & Ma, Y-Q. 1983, *ApJ*, 272, 317
- Martin, N. F., Ibata, R. A., Chapman, S. C., Irwin, M., & Lewis, G. F. 2007, *MNRAS*, 380, 281
- Martinez, G. D., Bullock, J. S., Kaplinghat, M., Strigari, L. E., & Trotta, R. 2009, *J. Cosmology Astropart. Phys.*, JCAP06(2009)014
- Moore, B., Ghigna, S., Governato, F., Lake, G., Quinn, T., Stadel, J., & Tozzi, P. 1999, *ApJ*, 524, L19
- Muñoz, R. R., *et al.* 2005, *ApJ*, 631, L137
- Muñoz, R. R., Carlin, J. L., Frinchaboy, P. M., Nidever, D. L., Majewski, S. R., & Patterson, R. J. 2006, *ApJ*, 650, L51
- Navarro, J. F., Frenk, C. S., & White, S. D. M. 1997, *ApJ*, 490, 493
- Palma, C., Majewski, S. R., Siegel, M. H., Patterson, R. J., Ostheimer, J. C., & Link, R. 2003, *AJ*, 125, 1352
- Piatek, S., Pryor, C., Armandroff, T. E., & Olszewski, E. W. 2002, *AJ*, 123, 2511
- Pieri, L., Lattanzi, M., & Silk, J. 2009, *MNRAS*, 399, 2033
- Robertson, B. E., & Zentner, A. R. 2009, *Phys. Rev. D*, 79, 083525
- Rolke, W. A., Lopez, A. M., & Conrad, J. 2005, *Nucl. Instrum. Meth.*, A551, 493
- Sánchez-Conde, M. A., Prada, F., Lokas, E. L., Gomez, M. E., Wojtak, R., & Moles, M. 2007, *Phys. Rev. D*, 76, 123509
- Servant, G., & Tait, T. M. P. 2003, *Nuclear Physics B*, 650, 391
- Shetrone, M. D., Côté, P., & Sargent, W. L. W. 2001, *ApJ*, 548, 592
- Siegel, M. H., Shetrone, M. D., & Irwin, M. 2008, *AJ*, 135, 2084
- Silk, J., & Stebbins, A. 1993, *ApJ*, 411, 439
- Spergel, D. N. *et al.* 2007, *ApJS*, 170, 377
- Strigari, L. E., Koushiappas, S. M., Bullock, J. S., & Kaplinghat, M. 2007, *Phys. Rev. D*, 75, 083526

- Strigari, L. E., Koushiappas, S. M., Bullock, J. S., Kaplinghat, M., Simon, J. D., Geha, M., & Willman, B. 2008, *ApJ*, 678, 614
- Taoso, M., Bertone, G., & Masiero, A. 2008, *J. Cosmology Astropart. Phys.*, JCAP03(2008)022
- Tyler, C. 2002, *Phys. Rev. D*, 66, 023509
- Walker, M. G., Mateo, M., Olszewski, E. W., Gnedin, O. Y., Wang, X., Bodhisattva, S., & Woodrooffe, M. 2007, *ApJ*, 667, L53
- Walker, M. G., Mateo, M., Olszewski, E. W., Penarrubia, J., Evans, N. W., & Gilmore, G. 2009, *ApJ*, 704, 1274
- Weekes, T. C. *et al.* (VERITAS collaboration) 2002, *Astropart. Phys.*, 17, 221
- Wilkinson, M. I., Kleyna, J. T., Evans, N. W., Gilmore, G. F., Irwin, M. J., & Grebel, E. K. 2004 *ApJ*, 611, L21
- Willman, B. *et al.* 2005, *ApJ*, 626, L85
- Wood, M. *et al.* 2008, *ApJ*, 678, 594
- York, D. G., *et al.* 2000, *AJ*, 120, 1579

Table 3: Results of observations of dSphs by VERITAS.

Quantity	Draco	Ursa Minor	Boötes 1	Willman 1
Exposure [s]	66185	68080	51532	49255
On Source [counts]	305	250	429	326
Total Background [counts]	3667	3084	4405	3602
Number of Background Regions	11	11	11	11
Significance <sup>a</sup>	-1.51	-1.77	1.35	-0.08
95% C.L. [counts] <sup>b</sup>	18.8	15.6	72.0	36.7
Average Effective Area [cm <sup>2</sup> ]	$5.84 \times 10^8$	$5.71 \times 10^8$	$6.37 \times 10^8$	$6.37 \times 10^8$
Energy Threshold [GeV] <sup>c</sup>	340	380	300	320
Flux Limit 95% C.L. [cm <sup>-2</sup> s <sup>-1</sup> ]	$0.49 \times 10^{-12}$	$0.40 \times 10^{-12}$	$2.19 \times 10^{-12}$	$1.17 \times 10^{-12}$

<sup>a</sup> Li and Ma method (Li & Ma 1983).

<sup>b</sup>Rolke method (Rolke *et al.* 2005).

<sup>c</sup>Definition given in text.

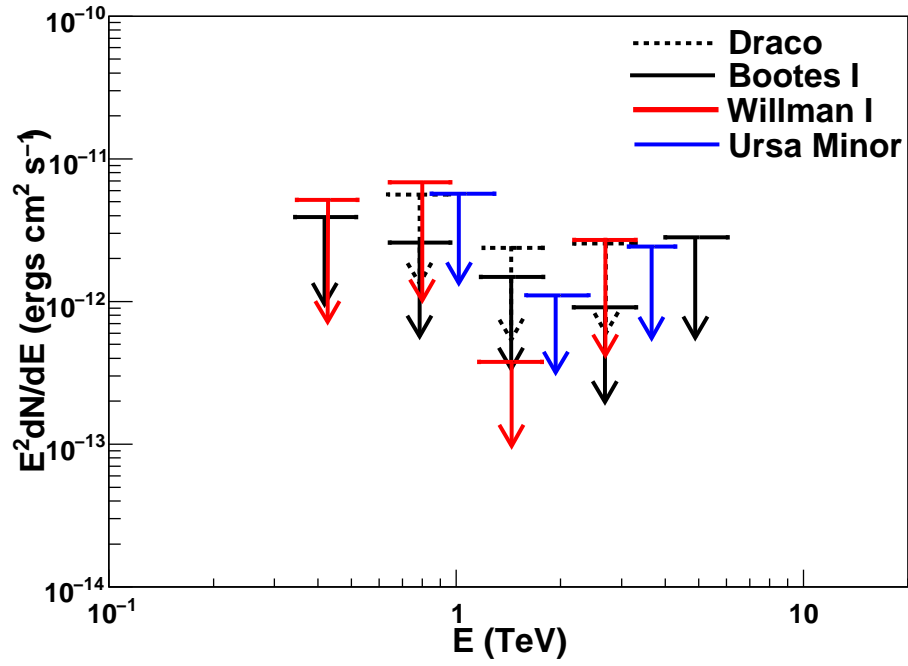


Fig. 1.— 95% C.L. upper limits on the spectral energy density ( $\text{erg cm}^{-2} \text{s}^{-1}$ ) as a function of gamma-ray energy for the four dSphs.

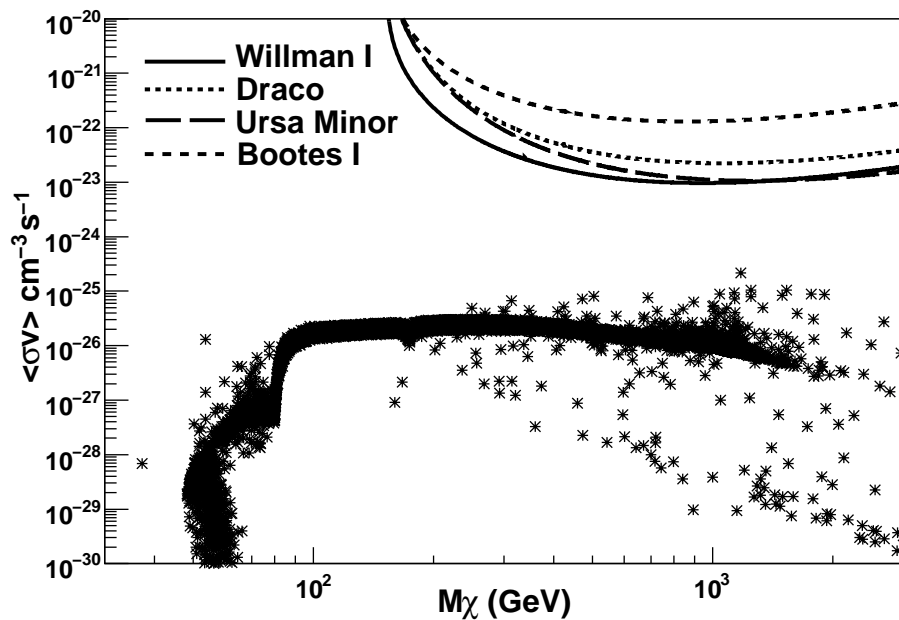


Fig. 2.— Exclusion regions in the  $(M_\chi, \langle\sigma v\rangle)$  parameter space based on the results of the observations. It is computed according to eq. 4 using a composite neutralino spectrum (see Wood *et al.* (2008)) and the values of  $J$  from Table 1. Black asterisks represent points from MSSM models that fall within  $\pm 3$  standard deviations of the relic density measured in the 3 year WMAP data set (Spergel *et al.* 2007).